ISSN 0024-4902, Lithology and Mineral Resources, 2023, Vol. 58, No. 4, pp. 273–290. © Pleiades Publishing, Inc., 2023.
Russian Text © The Author(s), 2023, published in Litologiya i Poleznye Iskopaemye, 2023, No. 4, pp. 319–337.

Structural Heterogeneity and Crystallinity Indices of Natural Kaolinites

B. A. Sakharov[a], * and V. A. Drits[a], **

[a] *Geological Institute, Russian Academy of Sciences, Moscow, 119017 Russia*

**e-mail: sakharovba@gmail.com*

***e-mail: victor.drits@mail.ru*

Received October 26, 2022; revised October 26, 2022; accepted January 9, 2023

Abstract—To overcome the existing uncertainty in the interpretation of kaolinite "crystallinity" indices (KCLs), such as HI (Hinckley, 1963), IK (Stoch, 1974; Stoch and Sikora, 1966), QF (Range and Weiss, 1969), AGFI (Aparicio and Galán, 1999; Aparicio et al., 2006), and WIRI (Chmielová and Weiss, 2002). Their values obtained for a representative collection of 30 kaolinite samples were compared with the results of modeling the corresponding X-ray diffraction patterns. It is shown that all the studied samples comprise a mixture of almost defect-free high-ordered kaolinite (HOK) and defective low-ordered kaolinite (LOK) phases. The HOK content shows correlation with the crystallinity index values described by different regression equations. The correlation is most prominent for HOK and the Hinckley index (HI), which is described by the quadratic equation HOK (%) = 12.236 HI^2 + 25.464 HI − 1.2622 with the correlation factor R^2 = 0.993. The obtained equations can be used to find HOK and LOK concentrations in natural kaolinites. Comparison of the structural parameters of defective kaolinites obtained by modeling their XRD patterns with those of Expert System (Plançon and Zacharie, 1990) showed that the latter sometimes predicts: (1) one-phase highly defective kaolinites, whereas their diffraction pattern modeling establishes a mixture of HOK and LOK phases; and (2) in two-phase samples, the content of the low-defect phase (ldp) is greater than 100%.

Keywords: kaolinite, defective structure, modeling of X-ray diffraction patterns, crystallinity indices

DOI: 10.1134/S0024490223700116

INTRODUCTION

Kaolinite $Al_2Si_2O_5(OH)_4$ is a dioctahedral mineral, with the layer structure consisting of one octahedral Al–O(OH) and one tetrahedral Si–O sheets (1 : 1) related to each other in a kaolinite layer via the apical oxygen atoms of tetrahedra. The adjacent kaolinite layers are united in the kaolinite structure due to the hydrogen bonds of OH groups located on the basal octahedral surface of one layer with oxygen atoms forming the basal tetrahedral surface of the adjacent layer. In the octahedral sheet of the kaolinite layer, three different cationic octahedral sites (A, B, and C), one of which is vacant and the other two are occupied by Al cations, differ in the arrangement of OH groups and oxygen atoms. In the base-centered unit cell of kaolinite described in (Bailey, 1993), the tetrahedral sheet is located at the 1 : 1 layer base, and the vacant position B is located on the long diagonal of the unit cell. Thus, the defect-free kaolinite has a one-layer triclinic (1Tc) structure and represents a regular alternation of layers related by simple translation (Bish and von Dreele, 1989).

Most varieties of natural kaolinites there are characterized by defective structure (Bailey, 1988; Brindley et al., 1986). In (Bookin et al., 1989) based on a comprehensive analysis of possible defects in the kaolinite structure, it was concluded that distortions of the real structure of 1 : 1 layers do not allow stacking faults, such as the mutual rotation of layers by 120°, the layer displacements by $b/3$, and the model of alternating layers with different positions of the octahedral vacancy proposed in (Brindley and Robinson, 1946; Murray, 1954; Plançon and Tchoubar, 1977). According to (Bookin et al., 1989), periodicity of a two-dimensional kaolinite layer can be described both as an orthogonal cell $\{a_0, b_0, \gamma_0\}$ ($\gamma_0 = 90°$) and as two enantiomorphic oblique cells $\{a_1, b_1, \gamma_1\}$ and $\{a_2, b_2, \gamma_2\}$ ($\gamma_{1,2} \neq 90°$), which are interrelated by a mirror plane passing through the vacant octahedron and the center of ditrigonal ring of the tetrahedral sheet of the kaolinite layer. Two enantiomorphic oblique cells and their corresponding vectors of interlayer translations t_1 and t_2, are interrelated by a mirror plane, make up a same defect-free structure of the right- and left-hand kaolinites indistinguishable by diffraction methods. The random alternation of vectors t_1 and t_2 inside indi-

vidual kaolinite crystallites will create right and left kaolinite structural fragments consisting of layers with the same type of vacancy and, thus, cause structural disorder in kaolinite. Due to the approximately trigonal symmetry of the kaolinite layer, a translation vector t_0 passing along the mirror plane can also exist in the kaolinite structure. Therefore, model of the defective kaolinite structure should be governed by the probability of layer translations W_{t1}, W_{t2}, and W_{t0}, respectively, which can be determined by careful modeling of the experimental diffraction pattern. Based on this model, experimental X-ray diffraction patterns (XRD) of natural kaolinites were simulated in (Drits et al., 2021; Plançon et al., 1989; Sakharov et al., 2016). It was shown that the studied samples consist of a physical mixture of two different populations of kaolinite crystallites with high-ordered (HOK) and low-ordered (LOK) structures occurring with different ratios in different samples.

Direct observation of stacking faults in the kaolinite structure was first carried out in (Kogure, 2011; Kogure and Inoue, 2005; Kogure et al., 2010). They demonstrated HRTEM images providing insight the types of these defects. The most common stacking faults were caused by the random alternative translations of kaolinite layer onto the translation vectors $t_1 \approx -a/3$ and $t_2 \approx a/6 - b/6$, which are interrelated by a pseudo-mirror plane passing through the vacant octahedron of the kaolinite layer. In some particles, the stacking faults were observed either as isolated insertions of single layers having an interlayer translation vector t_2 into an ordered sequence of layers with translation t_1 or as an alternation of two types of multilayer blocks comprising layers with translations t_1 or t_2. In particular, it turned out that the diagenetic kaolinite sample includes only defects related with the alternation of interlayer translations t_1 or t_2, but lacks defects related to the presence of layers with different positions of the octahedral vacancy or rotation of layers at $+/- n60°$. In contrast, the sedimentary kaolinite sample contains both types of defects, but defects of the second type (layers with different vacancies or mutual rotations) are extremely rare. These data fully confirmed the defect structure of kaolinite proposed in (Bookin et al., 1989).

Direct observation of the enantiomorphism of kaolinite crystals was established in (Samotoin, 2010, 2011; Samotoin and Bortnikov, 2011). Using the methods of vacuum Au decoration and transmission electron microscopy, they unraveled the existence of right- and left-handed kaolinite micro- and macrocrystals produced by ancient crust weathering.

Mathematical methods for modeling XRD patterns of defective layer crystals are complicated and, therefore, not used in conventional studies of kaolinites. To assess the perfection of kaolinite structure for both industrial purposes and geological tasks, the "crystallinity" indices are often used (Aparicio and Galán, 1999; Aparicio et al., 2006; Chmielová and Weiss, 2002; Hinckley, 1963; Range and Weiss, 1969; Stoch, 1974; Stoch and Sikora, 1966), based on simple measurements of X-ray diffraction peak heights measured in the region of 02*l* and 11*l* reflections as the most sensitive to structural defects. It is usually assumed that the kaolinite crystallinity indices (KCIs) evaluate some generalized degree of order-disorder in their structures, including a set of various defects. However, authors of the corresponding papers did not provide any justification for why certain measurements on XRD powder patterns are related to these coefficient-indices with parameters of the defective structure of kaolinites. Obviously, all these coefficients do not carry any physical meaning and are therefore empirical. They are used when it is not required to know the nature and distribution of defects in the kaolinite structure, but it is necessary to somehow discriminate the samples. It was noted for the first time in (Plançon et al., 1988) that the Hinckley crystallinity index (HI), in its classical sense, evaluates neither the types nor the number of different structural defects. However, this index is nonlinearly related to the proportions of two kaolinite types in the models of defect structures. At the same time, they did not establish the relationship of the HI index with the composition of real kaolinite samples, although it may be very important for a deeper understanding of the nature of these minerals.

In contrast to the crystallinity indices, the Expert system (Plançon and Zacharie, 1990) uses a set of relatively simple measurements on an experimental diffractogram to estimate some real structural parameters of natural kaolinites. In several publications (Aparicio and Galán, 1999; Aparicio et al., 2006; Chmielová and Weiss, 2002; González et al., 1999), a correlation has been established between the data of the Expert System and the kaolinite crystallinity indices. However, no wide comparison of both data with the results of modeling experimental XRD patterns was conducted.

In the present work, in addition to the studied collection of 18 kaolinite samples (Drits et al., 2021), 12 more samples were studied by modeling XRD patterns, with the determination of the content of HOK and LOK phases, as well as their structural parameters. For all 30 samples, we calculated different KCI values and their comparison with the HOK values. In addition, we analyzed all kaolinite samples using an Expert System (Plançon and Zacharie, 1990) and compared the obtained results with the data on modeling diffraction patterns.

MATERIALS AND METHODS

The collection of 18 previously studied kaolinite samples (Drits et al., 2021) was supplemented with 12 new samples (Keok1D, Keok2D, Keok3D, Keok4D, Kaol-3, Mag1, 5914, Ma-4, S218, 5920, Bor-2, and 6194), which, like the previous ones, were studied by

X-ray powder diffraction. The location of all samples and their genesis are given in Table 1. Samples Keok1D, Keok2D, Keok3D, and Keok4D were extracted from the geode by careful grinding and sieving through a <0.1 mm sieve. The remaining eight samples were not subjected to any pretreatment, except for short-term grinding with a rubber pestle in a small water volume, followed by the extraction of <0.001 mm fractions from suspension. All new samples contained insignificant amounts of impurities.

Powder diffractograms were obtained using a Bruker D-8 Advance X-ray diffractometer (Bruker AXS Corporation, Karlsruhe, Germany; 40 kV, 40 mA; Bragg–Brentano θ/θ configuration; goniometer radius 250 mm) equipped with a scintillation detector of Cu$K\alpha$ radiation in the 2θ range of 8°–65° at a scanning step of 0.05° 2θ. The high quality of diffractograms was provided by an exposure of 150 s per step, which significantly reduces random fluctuations in diffracted intensity. The horizontal and anti-scattering slits with fixed divergence for the incident beam had a width of 0.5°; for the diffracted beam, the receiving slit of detector was 0.04°; and the vertical divergence of both beams was limited by two 2.5° Soller slits. The flat rectangular sample holder (3.0 × 2.5 × 0.5 cm) and side-loading preparation significantly reduced the predominant orientation of particles.

RESULTS

Modeling of experimental X-ray diffraction patterns

A collection of 18 kaolinite samples of different genesis was studied by modeling the XRD patterns in (Drits et al., 2021). The results showed that the samples consist of two phases: high-ordered (HOK) and low-ordered (LOK) phases formed by the same B-vacant kaolinite layers, but differing sharply in the content of stacking faults. The HOK phase has an almost defect-free structure, in which 97–100% of layer pairs are connected by the translation vector t_1, and no more than 3% of layer pairs make up the enantiomorphic fragments with translations t_2 only in some samples. On the contrary, the LOK phase has a highly defective structure, in which three vectors of layer translations t_1, t_2, and t_0 randomly alternate in the following ratios W_{t1} (0.55–0.60) : W_{t2} (0.35–0.45) : W_{t0} (0–0.05). In addition to these structural defects, the LOK phase often contains "arbitrary" stacking faults (*Wa*) associated with random shifts of layers to arbitrary translations and/or with rotations of adjacent layers to arbitrary angles. However, the content of such defects in the LOK phase did not exceed 10%. The quality of coincidence between the calculated and experimental XRD patterns could be improved slightly due to defects associated with variations in the length of interlayer translations along the *a* and/or *c** axes in both HOK and LOK phases.

In this work, experimental diffraction patterns of 12 new kaolinite samples (Keok1D, Keok2D, Keok3D, Keok4D, Kaol-3, Mag1, 5914, Ma-4, S218, 5920, Bor-2, and 6194) were successfully modeled using the same two-phase model of the defective structure. The best agreement between the experimental and calculated diffraction patterns was achieved by the trial-and-error method when we changed both structural parameters of the HOK and LOK phases, as well as their content in the sample, and evaluated by the profile factor Rp (Table 2). The concentrations of layer translations W_{t1}, W_{t2}, and W_{t0} in the HOK and LOK phases in individual samples remained within the same values as in the previously studied samples (Drits et al., 2021). It can only be noted that for some new samples, the maximum content of arbitrary stacking faults (*Wa*) increased to 15% (Table 2).

The results of modeling experimental diffractograms of the entire collection of 30 kaolinite samples suggested the following conclusions. All samples turned out to be a mixture of HOK and LOK phases with their ratio varying from 86 : 14 to 4 : 96 (Table 2). Individual HOK and LOK phases in different samples do not differ too much from each other both in terms of the content of layer translations W_{t1}, W_{t2}, W_{t0}, and arbitrary stacking faults *Wa* (Table 2). Therefore, it can be assumed at the qualitative level, that both of these two phases do not change much in terms of the defect degree in different samples. Table 2 shows that sizes of the coherent scattering domains (CSD) in the plane of layers *ab*, *D*, and the total number of layers in crystallites (*N*) for HOK and LOK phases are usually the same or very close for the same sample. Finally, the degree of particle orientation (α) corresponding to different HOK and LOK populations in the same sample is also the same or very close (Table 2). All these features of the real structure of kaolinite samples indicate that the ratio of HOK and LOK phases is the main factor that governs intensity distribution in the diffraction pattern. At the same time, as shown in (Drits et al., 2021; Plançon et al., 1989; Sakharov et al., 2016), HOK crystallites make the main contribution to the position, width, and intensity of 02*l* and 11*l* reflections at 2θ = 19.0°–24.5°, whereas LOK crystallites contribute only to background scattering as a wide and asymmetrical "hump" and to the reflection profile 020. In Fig. 1a, the comparison of fragments of an experimental diffractogram in this angular region for sample G5 and the diffractograms calculated for an optimal mixture of HOK and LOK phases shows the best correspondence of diffraction patterns. The lower part of Fig. 1a shows the corresponding contributions of the HOK and LOK phases to the resulting diffraction pattern.

Table 1. Location and genesis of the studied samples

No.	Sample	Genesis	Deposit
1	Keok-1	Hydrothermal	Warsaw geode, Keokuk, Iova, USA
2	Keok-2	Hydrothermal	Warsaw geode, Keokuk, Iova, USA
3	Keok1D	Hydrothermal	Warsaw geode, Keokuk, Iova, USA
4	Keok2D	Hydrothermal	Warsaw geode, Keokuk, Iova, USA
5	Keok3D	Hydrothermal	Warsaw geode, Keokuk, Iova, USA
6	Ch-76	Sedimentary	Coal deposits, Shanxi province, northern China
7	Keok4D	Hydrothermal	Warsaw geode, Keokuk, Iova, USA
8	Keok-3	Hydrothermal	Warsaw geode, Keokuk, Iova, USA
9	E-4	Weathering	Elenin deposit, granite remnant, Ukraine
10	Keok-4	Hydrothermal	Warsaw geode, Keokuk, Iova, USA
11	An	Weathering	Angren deposit, remnants of felsic effusive and extrusive rocks, Uzbekistan
12	Dec	Hydrothermal	From veins, Decazeville, France
13	Pr	Weathering	Prosvyanov deposit, granite remnant, Dnepropetrovsk region, Ukraine
14	Ch-67	Hydrothermal	Suzhou, China
15	Sd	Weathering	Sedlets deposit, granite remnant, Czech Republic
16	Vl	Weathering	Vladimir deposit, Ukraine
17	KGa-1b	Weathering	CMS, Warren County, Georgia, USA
18	Sm	Weathering	Smolyansk deposit, Ukraine
19	Kaol-3	Unknown	Unknown
20	KGa-1	Weathering	CMS, Warren County, Georgia, USA
21	Mag1	Weathering	Eleninsk deposit, Magnitogorsk
22	G-5	Weathering	Warren County, Georgia, USA
23	Im	Weathering	'Hywite Alum' raw kaolinite ("ball clay") from Devon (Imerys, UK)
24	MA4	Sedimentary	Shulepovo deposit, Ryazan
25	5914	Sedimentary	Shulepovo deposit, Ryazan
26	S218	Sedimentary	Shulepovo deposit, Ryazan
27	5920	Sedimentary	Shulepovo deposit, Ryazan
28	6194	Sedimentary	Shulepovo deposit, Ryazan
29	Bor-2	Sedimentary	Borovichi deposit, Tver region
30	KGa-2	Weathering	CMS, Warren County, Georgia, USA

Measurements on diffractograms required to determine the crystallinity indices and structural parameters of Expert System

To reliably determine the crystallinity indices and structural parameters of the Expert System, it is necessary to have a high quality diffraction pattern with minimized fluctuations of the diffracted intensity and to unify the procedure of all measurements on the diffractogram. The high quality of diffraction pattern is achieved by long-term exposure at each scanning step and, as a rule, is chosen experimentally for each specific design of the diffractometer. In the case of our device equipped with a scintillation detector, exposure time was 150 s at the measurement point. We used EXCEL spreadsheets for specific measurements on the diffractogram. After normalizing all intensities of the experimental diffraction pattern to its maximum value taken as 100, we determined the minimum values for constructing the necessary background lines and the maximum values for finding the corresponding reflection peak positions. For each background line, we obtained a straight-line equation, which was used to calculate the peak heights needed to calculate the crystallinity indices or structural parameters of Expert System. To determine the full width of diffraction peaks at half maximum (FWHM), values of the corresponding intensities were found by approximating with straight lines the experimental points on the left and right "slopes" from its maximum. The EXCEL plot with a diffraction pattern, background

Table 2. Contents of the high-ordered (HOK) and low-ordered (LOK) phases and their structural parameters obtained by modeling diffraction patterns of natural kaolinites

No.	Sample	Phase	C, %	W_{t1}	W_{t2}	W_{t0}	W_a	N	D, Å	α, degr.	Rp, %
1	Keok-1	HOK	86	1	0	0	0	80	100–1100	90	18.8††
		LOK	14	0.55	0.45	0	0	60	100–1100	80	
2	Keok-2	HOK	80	1	0	0	0	50	100–1000	150	15.8††
		LOK	20	0.55	0.45	0	0	50	100–1000	150	
3	Keok1D	HOK	80	1	0	0	0	65	100–1100	120	20.0††
		LOK	20	0.55	0.45	0	0.10	65	100–1100	120	
4	Keok2D	HOK	80	1	0	0	0	65	100–1100	120	~20.0††
		LOK	20	0.55	0.45	0	0	65	100–1100	120	
5	Keok3D	HOK	77	0.99	0.01	0	0	65	100–1100	120	20.1††
		LOK	23	0.55	0.45	0	0	65	100–1100	120	
6	Ch-76	HOK	76	1	0	0	0	35	100–900	110	11.1
		LOK	24	0.55	0.45	0	0.10	35	100–900	110	
7	Keok4D	HOK	73	0.99	0.01	0	0	65	100–1100	120	19.3††
		LOK	27	0.55	0.45	0	0	65	100–1100	120	
8	Keok-3	HOK	69	0.98	0.02	0	0	60	100–1100	90	11.6
		LOK	31	0.55	0.45	0	0	60	100–1100	90	
9	E-4	HOK	68	0.98	0.02	0	0	65	100–1000	140	8.3
		LOK	32	0.55	0.45	0	0	65	100–1000	140	
10	Keok-4	HOK	68	1	0	0	0	50	100–800	120	11.6
		LOK	32	0.55	0.45	0	0	50	100–800	120	
11	An	HOK	63	0.98	0.02	0	0	28	100–900	70	11.7
		LOK	37	0.55	0.43	0.02	0.05	28	100–900	70	
12	Dec	HOK	55	0.98	0.02	0	0	50	100–900	120	9.8
		LOK	45	0.55	0.45	0	0	50	100–900	120	
13	Pr	HOK	55	0.98	0.02	0	0	18	100–900	60	11.7
		LOK	45	0.55	0.43	0.02	0.05	18	100–900	60	
14	Ch-67	HOK	54	0.98	0.02	0	0	30	100–900	100	9.3
		LOK	46	0.55	0.45	0	0.04	30	100–900	100	
15	Sd	HOK	41	0.98	0.02	0	0.06	18	100–900	75	10.3
		LOK	59	0.60	0.38	0.02	0.05	18	100–900	75	
16	Vl	HOK	37	0.98	0.02	0	0	18	100–700	90	9.7
		LOK	63	0.55	0.43	0.02	0.05	18	100–700	90	
17	KGa-1b	HOK	37	0.98	0.02	0	0	25	100–800	160	10.3
		LOK	63	0.55	0.45	0	0.04	25	100–800	160	
18	Sm	HOK	36	0.97	0.03	0	0	18	100–700	180	9.3
		LOK	64	0.55	0.43	0.02	0.05	18	100–700	180	
19	Kaol-3	HOK	36	0.98	0.02	0	0.03	18	100–900	65	15.6††
		LOK	64	0.60	0.35	0.05	0.10	18	100–900	65	
20	KGa-1	HOK	27	0.97	0.03	0	0	45	200–800	90	10.0
		LOK	73	0.58	0.37	0.05	0.05	45	200–800	90	
21	Mag1	HOK	23	0.98	0.02	0	0	14	100–700	70	11.3
		LOK	77	0.55	0.40	0.05	0.10	14	100–600	70	

Table 2. (Contd.)

No.	Sample	Phase	C, %	W_{t1}	W_{t2}	W_{t0}	W_a	N	D, Å	α, degr.	Rp, %
22	G-5	HOK	18	0.98	0.02	0	0	18	100–700	110	11.3
		LOK	82	0.55	0.40	0.05	0.05	18	100–700	110	
	G-5†	LOK	100	0.75	0.20	0.05	0.05	18	100–700	110	11.3
23	Im	HOK	18	0.98	0.02	0	0	18	100–700	100	11.0
		LOK	82	0.55	0.43	0.02	0.05	18	100–700	100	
24	Ma-4	HOK	15	0.98	0.02	0	0	12	100–700	110	10.8
		LOK	85	0.55	0.35	0.10	0.10	12	100–700	90	
25	5914	HOK	13	0.98	0.02	0	0	11	100–800	50	10.6
		LOK	87	0.55	0.35	0.10	0.15	11	100–800	60	
26	S218	HOK	12	0.98	0.02	0	0	11	100–800	57	11.2
		LOK	88	0.55	0.35	0.10	0.10	11	100–800	57	
27	5920	HOK	12	1	0	0	0	11	100–800	70	12.1
		LOK	88	0.55	0.35	0.10	0.15	11	100–800	70	
28	6194	HOK	9	0.98	0.02	0	0	10	100–700	70	14.3
		LOK	91	0.55	0.35	0.10	0.10	10	100–700	70	
29	Bor-2	HOK	6	0.98	0.02	0	0	9	100–800	60	12.4
		LOK	94	0.65	0.25	0.10	0.15	9	100–800	55	
30	KGa-2	HOK	4	0.98	0.02	0	0	20	100–700	120	10.9
		LOK	96	0.58	0.37	0.05	0.07	20	100–700	120	

W_{t1}, W_{t2}, W_{t0}—probabilities of layer translations $t_1 = -0.2200a_0 + 0.1722b_0$, $t_2 = -0.2200a_0 - 0.1722b_0$, and $t_0 = 0.3698a_0$ (Drits et al., 2021) in the defect structure of kaolinite; W_a—probability of arbitrary stacking defects; N—average number of layers in crystals; D—dimensions of the coherent scattering domains on *ab* plane of crystal, defined by the uniform distribution from the minimum to maximum value; α—parameter of a Gaussian function describing the particle orientation in sample; Rp—profile factor characterizing the degree of inconsistency between the experimental and calculated diffraction patterns; †—structural parameters of the one-phase model; ††—high Rp values are related to impurities whose diffraction patterns were not modeled.

lines, and peak widths served as a test of measurements. As an example, Figs. 1b–1d shows fragments of the diffraction pattern of sample G5 and the corresponding measurements on them for calculating the crystallinity indices HI, QF, and IK, respectively.

According to (Aparicio, et al., 2006; Chmielová and Weiss, 2002), the determination of crystallinity indices AGFI and WIRI requires first the mathematical decomposition of the diffraction profile in the region of 02*l* and 11*l* reflections to individual maxima using a Pearson VII function and an asymmetric Pearson VII function, respectively, and the subsequent determination of peak intensities. Their FWHM values are also needed for calculating the WIRI value. All necessary calculations in this work were carried out using the Fytik software (Wojdyr, 2010). Figures 1e and 1f show examples of the diffraction profile decomposition for sample G5 to find the crystallinity indices AGFI and WIRI. It should be noted that the EXCEL spreadsheet constructed for one sample and the corresponding crystallinity index can be used for another sample, replacing only the corresponding equations of background lines. Only sometimes, small changes in the minimum values may be required to correct the background lines or maximum values for the positions of diffraction peaks.

Determination of kaolinite crystallinity indices

The *Hinckley index* (Hinckley, 1963) is the most common empirical parameter that is widely used to assess the perfection degree of various kaolinites. On the powder diffractogram (Fig. 1b), intensities of $1\bar{1}0$ and $11\bar{1}$ reflections (denoted as A and B, respectively) are measured relative to the background line drawn between the bases of these peaks; the intensity of $1\bar{1}0$ reflection (denoted as C) is measured relative to the background line of the entire diffractogram; then the ratio (A + B)/C is calculated. According to the literature data, this dimensionless number or the Hinckley "crystallinity" index denoted as HI varies from ~0.2 to ~1.7 for natural kaolinites. The higher the HI value, the higher the perfection degree of the kaolinite structure.

As noted in (Drits et al., 2021; Plançon et al., 1989; Sakharov et al., 2016), the HOK phase in the region of 02*l* and 11*l* reflections contributes mainly to their intensities, whereas the notable background separating these reflections from the general background line of

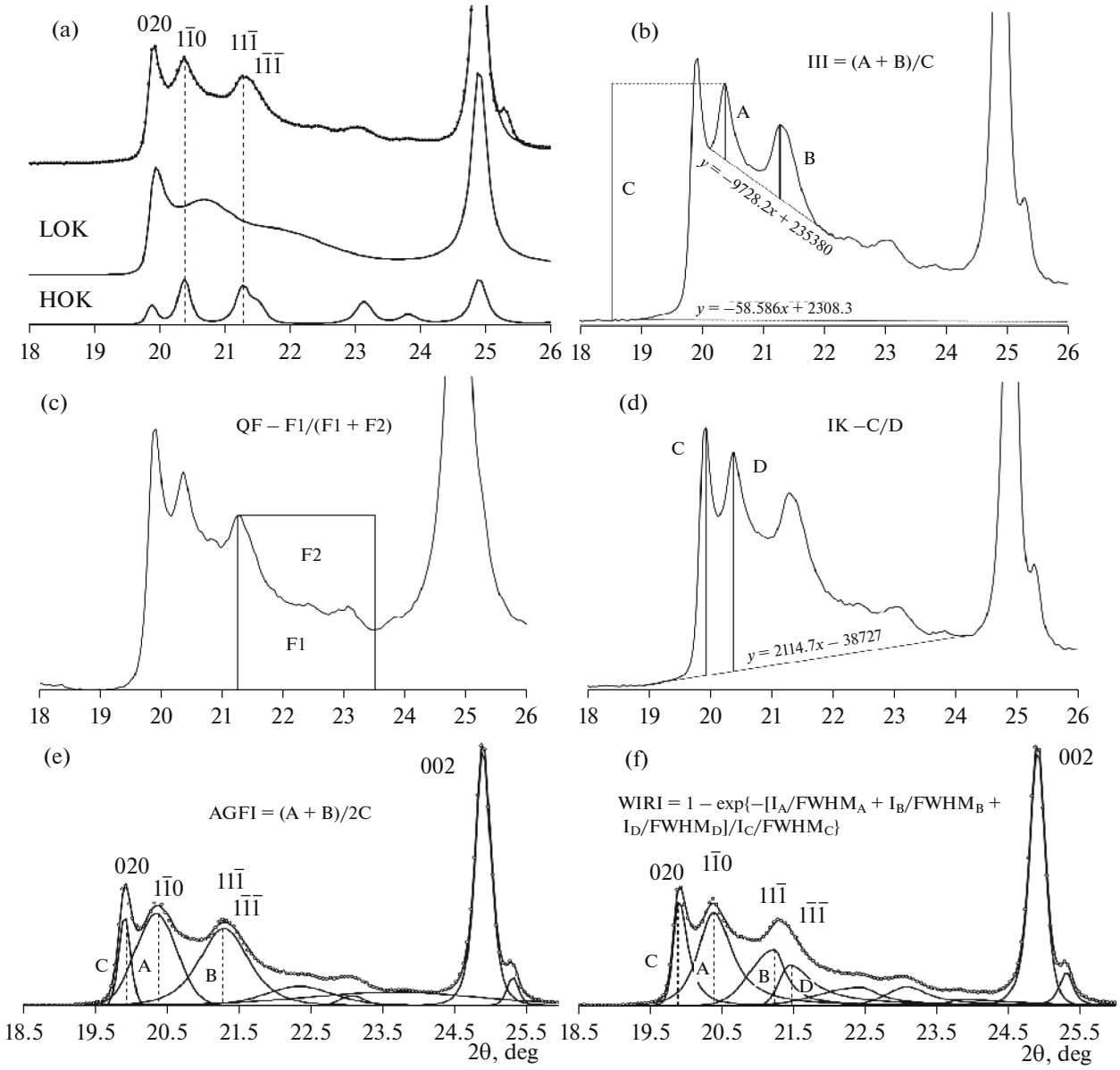

Fig. 1. Determination of structural defects in kaolinites by the diffraction pattern modeling (a) and the "crystallinity" indices (b–f): HI (Hinckley, 1963) (b), QF (Range and Weiss, 1969) (c), IK (Stoch, 1974) (d), AGFI (Aparicio et al., 2006) (e), WIRI (Chmielová and Weiss, 2002) (f); I_A, I_B, I_D, I_C, FWHM$_A$, FWHM$_B$, FWHM$_D$, FWHM$_C$—intensities of peaks A, B, D, and C and their corresponding peak widths at half width.

the diffractogram is the a result of the contribution of the LOK phase. In fact, the Hinckley index evaluates in a simplified way the HOK phase contribution to total intensity of the diffractogram by calculating the ratio of the sum of $1\bar{1}0$ and $11\bar{1}$ reflections belonging to the HOK phase relative to the sum of the intensities from $1\bar{1}0$ reflection of the HOK phase and the background from the LOK phase. Table 2 shows the HOK and HI values for the studied samples. It turned out that the Hinckley index and the HOK phase content shows a correlation described well by the quadratic equation

$$\text{HOK}\ (\%) = 12.236\ \text{HI}^2 + 25.464\ \text{HI} - 1.2622 \quad (1)$$

with correlation factor $R^2 = 0.993$ (Fig. 2). It should be noted that the regression curve is very close to the origin—the point for which the HI and HOK values should be zero. It is obvious that now the Hinckley index acquires a certain meaning via the HOK value. By calculating HI for the studied kaolinite and using Eq. (1), it is possible to obtain an important structural parameter (HOK), indicating the ratio of defective (LOK) and almost defect-free (HOK) crystallites in the sample.

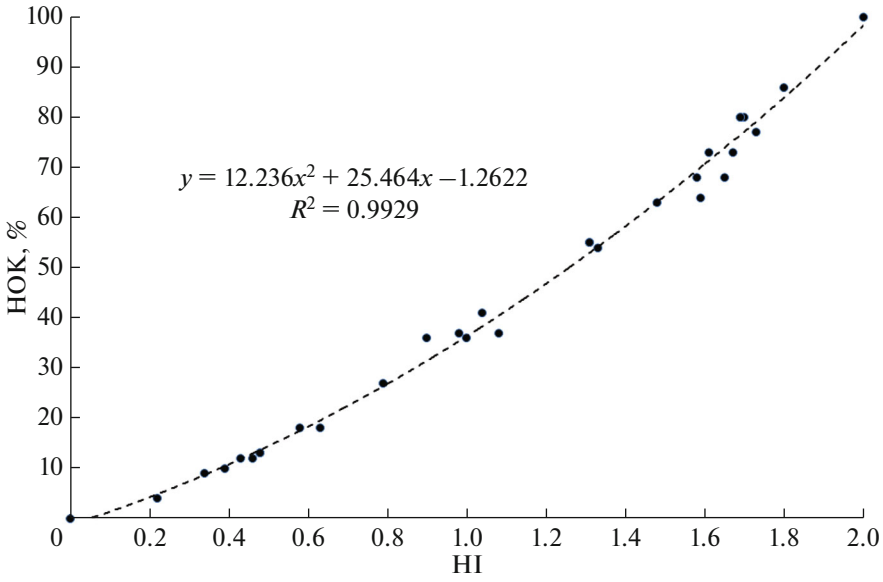

Fig. 2. Relationship between HOK and Hinckley crystallinity index (HI).

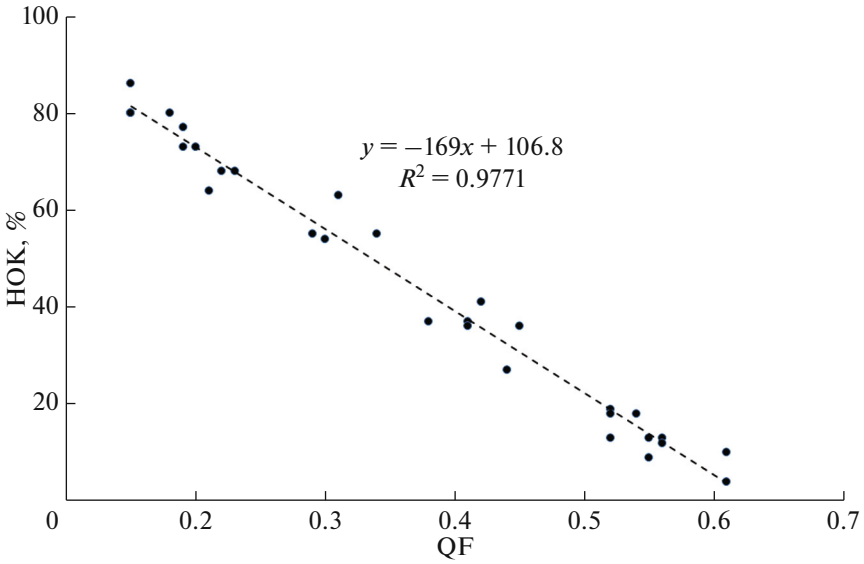

Fig. 3. Relationship between HOK and QF index.

The *kaolinite crystallinity index QF* (Range and Weiss, 1969) is another simple and widely used empirical parameter for assessing the perfection degree of kaolinite samples. It calculates the ratio of the area under the diffraction pattern between $11\bar{1}$ and $02\bar{1}$ reflections (F_1, Fig. 1c) to the area of the rectangle formed by the peak $11\bar{1}$ heights and the distance from its top to peak $02\bar{1}$ as the base ($F_1 + F_2$, Fig. 1c). It is believed that kaolinites with QF = 0.20–0.45 are low defective, kaolinites with QF = 0.45–0.60 are medium defective, and kaolinites with QF > 0.60 are highly defective (Aparicio et al., 1999; Chmielová and Weiss, 2002; González et al., 1999). The HOK vs. QF correlation is described by a linear equation

$$\text{HOK}\ (\%) = -169\ \text{QF} + 106.8 \qquad (2)$$

with $R^2 = 0.977$ (Fig. 3).

The *kaolinite crystallinity index IK* (Stoch, 1974; Stoch and Sikora, 1966) uses the intensity ratio of reflections 020 (C, Fig. 1d) and $1\bar{1}0$ (D, Fig. 1d). Usually, its value ranges from 0.4 to 1.4 and it is considered that the

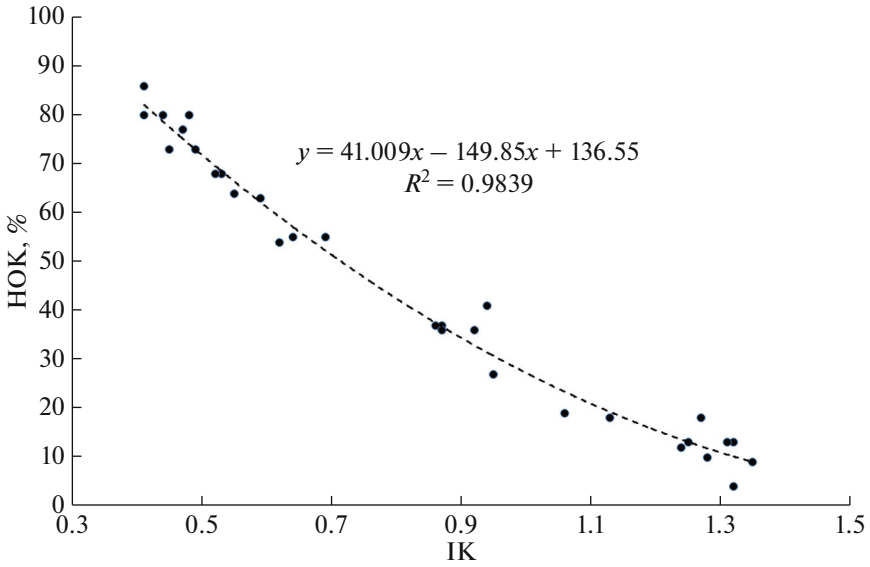

Fig. 4. Relationship between HOK and IK.

disordered and ordered kaolinites have IK > 1.0 and <0.7, respectively. Figure 4 shows the HOK/IK correlation described by the quadratic equation

$$\text{HOK}\ (\%) = 41.009\,\text{IK}^2 - 149.85\,\text{IK} + 136.55 \quad (3)$$

with $R^2 = 0.98$. Equations (2) and (3) can be used to find the HOK phase content in samples for which the QF and IK values are measured.

Unlike all previous crystallinity indices, the *kaolinite crystallinity index AGFI* (Aparicio and Galán, 1999; Aparicio et al., 2006) uses the decomposition of the diffraction profile in the region of 02*l* and 11*l* reflections into individual maximums using the Pearson VII function. Measuring the heights A, B, and C of $1\bar{1}0$, $11\bar{1}$, and 020 reflections, one can calculate the ratio AGFI = (A + B)/2C (Fig. 1e). This index was developed and used by the authors for kaolinite samples containing impurities of quartz, feldspar, illite, smectite, chlorite, halloysite, iron hydroxides, and amorphous silica. However, it should be noted that decomposition of the diffraction profile into individual maximums is not always unambiguous and exclusive, since the number of peaks and the position of some of them may be unknown. Moreover, for a complex profile composed, as we now know, of contributions from the HOK and LOK phases (Fig. 1a), any decomposition into individual peaks described by the Pearson VII function will be incorrect. Nevertheless, the HOK vs. AGFI correlation is described well by the quadratic equation

$$\text{HOK}\ (\%) = 20.632\,\text{AGFI}^2 + 105.75\,\text{AGFI} - 54.801 \quad (4)$$

with $R^2 = 0.98$ (Fig. 5). At the same time, if we assume that HOK = 100% for the Keokuk sample (Bish and von Dreele, 1989) whose structure was refined by the Rietveld method, corresponding measurements on its diffractogram yield AGFI = 2.56, and AGFI = 6.32, according to Eq. 4. However, if we approximate the experimental points in Fig. 5 with a linear equation instead of quadratic equation,

$$\text{HOK}\ (\%) = 42.438\,\text{AGFI} - 14.385 \quad (5)$$

with $R^2 = 0.935$ (Fig. 5), then, according to Eq. 5, the value of HOK = 100% is achieved at AGFI = 2.69, which is significantly closer to the measured value of AGFI = 2.56 than for the quadratic equation.

The *kaolinite crystallinity index WIRI*, i.e., weighing intensity ratio index proposed in (Chmielová and Weiss, 2002) represents a modified AGFI version including 020, $1\bar{1}0$, $11\bar{1}$, as well as $1\bar{1}\bar{1}$ reflections in the case of kaolinites, in which the latter reflection is manifested in the diffraction pattern. In addition, these authors normalized intensities 020, $1\bar{1}0$, $11\bar{1}$, and $1\bar{1}\bar{1}$ reflections to their corresponding FWHM values as the products of coefficients $w_1 = 1/\text{FWHM}(020)$, $w_2 = 1/\text{FWHM}(1\bar{1}0)$, $w_3 = 1/\text{FWHM}(11\bar{1})$, and $w_4 = 1/\text{FWHM}(1\bar{1}\bar{1})$. They also used an expression for the exponent so that the WIRI values vary between 0 and 1:

$$\text{WIRI} = 1 - \exp\{-[w_1 I(1\bar{1}0) + w_2 I(11\bar{1}) + w_3 I(1\bar{1}\bar{1})]/w_4 I(020)\}. \quad (6)$$

In this paper, the diffraction profile was decomposed using the asymmetric Split Pearson VII function. If we construct the AGFI vs. WIRI correlation (Table 3), including all data for the samples studied in this paper, as well as samples studied in (Chmielová and Weiss,

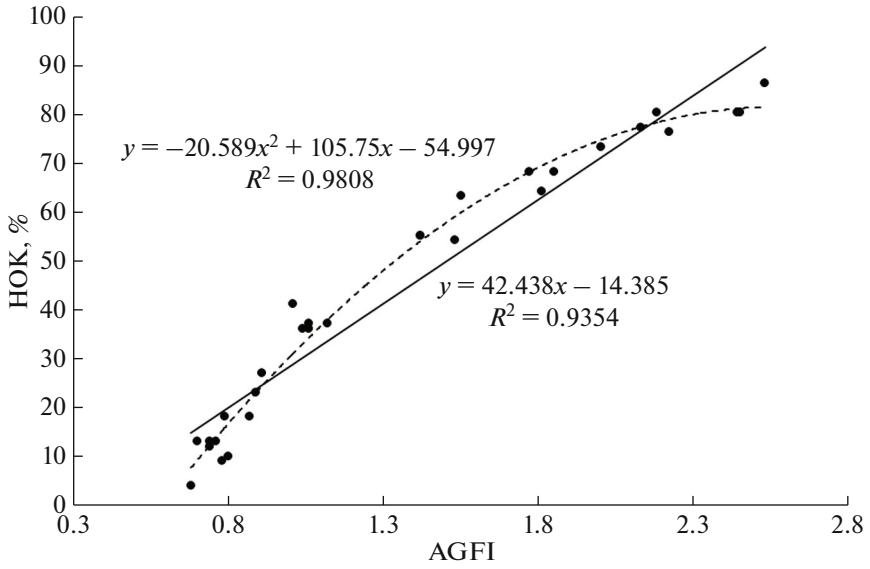

Fig. 5. Relationship between HOK and crystallinity index AGFI.

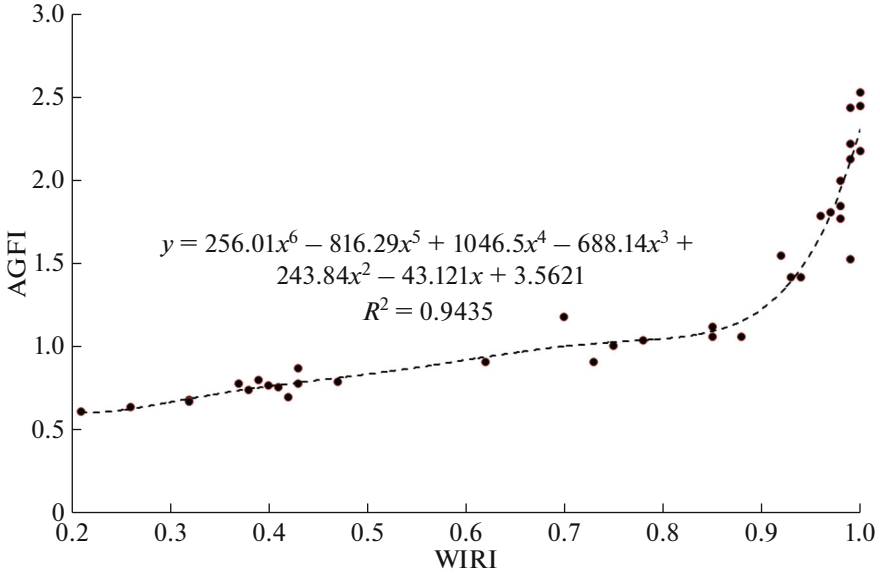

Fig. 6. Relationship between crystallinity indices AGFI and WIRI.

2002, Table 4), then it is described well by the sextic equation

$$\begin{aligned}\text{AGFI} = {} & 256.01\,\text{WIRI}^6 - 816.29\,\text{WIRI}^5 \\ & + 1046.5\,\text{WIIRI}^4 - 688.14\,\text{WIIRI}^3 \\ & + 243.84\,\text{WIIRI}^2 \\ & - 243.121\,\text{WIRI} + 3.5621\end{aligned} \quad (7)$$

with $R^2 = 0.94$ (Fig. 6). A similar correlation of HOK and WIRI values is described by the quintic equation

$$\begin{aligned}\text{HOK}\,(\%) = {} & 2119.3\,\text{WIRI}^5 \\ & - 5258.5\,\text{WIIRI}^4 + 4982.6\,\text{WIIRI}^3 \\ & - 2313.0\,\text{WIIRI}^2 + 621.27\,\text{WIRI} - 72.759\end{aligned} \quad (8)$$

with $R^2 = 0.955$ (Fig. 7).

Expert System (Plançon and Zacharie, 1990)

In contrast to the empirical crystallinity indices HI, QF, IK, AGFI, and WIRI, the Expert System is

Table 3. Content of the high-ordered HOK phase in natural kaolinites and corresponding crystallinity indices HI, QF, IK, AGFI, WIRI and ldp values characterizing the content of low-defect phase, according to Expert System

No.	Sample	HOK	HI	QF	IK	AGFI	WIRI	ldp
1	Keok-1	86	1.80	0.15	0.41	2.53	1	113
2	Keok-2	80	1.70	0.18	0.44	2.44	0.99	105
3	Keok1D	80	1.69	0.15	0.41	2.45	1	89
4	Keok2D	80	1.69	0.15	0.48	2.18	1	86
5	Keok3D	77	1.73	0.19	0.47	2.13	0.99	86
6	Ch-76	76	1.67	0.2	0.45	2.22	0.99	86
7	Keok4D	73	1.61	0.19	0.49	2	0.98	72
8	Keok-3	69	1.59	0.21	0.55	1.81	0.97	70
9	E-4	68	1.58	0.23	0.53	1.77	0.98	61
10	Keok-4	68	1.65	0.22	0.52	1.85	0.98	59
11	An	63	1.48	0.31	0.59	1.55	0.92	42
12	Dec	55	1.31	0.29	0.64	1.42	0.93	43
13	Pr	55	1.31	0.34	0.69	1.42	0.94	43
14	Ch-67	54	1.33	0.3	0.62	1.53	0.99	37
15	Sd	41	1.04	0.42	0.94	1.01	0.75	36
16	Vl	37	1.08	0.41	0.87	1.12	0.85	15
17	KGa-1b	37	0.98	0.38	0.86	1.06	0.85	0
18	Sm	36	0.90	0.45	0.92	1.04	0.78	13
19	Kaol-3	36	1.00	0.41	0.87	1.06	0.88	0
20	KGa-1	27	0.79	0.44	0.95	0.91	0.73	40
21	Mag1	23	0.64	0.52	1.06	0.89	0.76	0
22	G-5	18	0.63	0.52	1.13	0.87	0.43	11
23	Im	18	0.58	0.54	1.27	0.79	0.47	0
24	MA4	15	0.48	0.52	1.32	0.7	0.42	102
25	5914	13	0.48	0.55	1.25	0.76	0.41	112
26	S218	12	0.46	0.56	1.24	0.74	0.52	94
27	5920	12	0.43	0.56	1.31	0.74	0.38	87
28	6194	9	0.34	0.55	1.35	0.78	0.43	0
29	BOR-2	6	0.39	0.61	1.28	0.8	0.39	9
30	KGa-2	4	0.22	0.61	1.32	0.68	0.32	0

based on a systematic analysis of numerous diffraction patterns calculated by the authors for structural models including various types of defects in the kaolinite structure. This system assumes the measurement on an experimental diffractogram of seven parameters in the region of 02*l* and 11*l* reflections and four parameters in the region of 20*l* and 13*l* reflections designated in Figs. 8a and 8b or in (Plançon and Zacharie, 1990, Figs. 1a, 1b) by numbers from 1 to 7 and from 8 to 11, respectively. Depending on their values, the computer program (expkaol.com) determines whether the given sample is one-phase or two-phase. For a two-phase sample, the program calculates the content (in %) of a well-crystallized kaolinite phase (Wp). In (Plançon and Zacharie, 1990), this phase is designated as ldp (low defect phase). In terms of structure, the ldp phase is similar to the HOK phase, since it has $W_{t1} : W_{t2} = 0.98 : 0.02$ (Plançon et al., 1989). Therefore, we will use hereafter the ldp designation instead of Wp. In the case of a one-phase sample, the system calculates the proportion of translation defects (p), the content of layers with a vacancy in the octahedral site C (W_C), the average number of layers in crystallites (N), and the value of translation length variations around the average value (δ). All crystals of one-phase samples established in (Plançon and Zacharie, 1990) contained relatively high concentrations of stacking faults and, therefore, should be considered as low order phases.

Application of this approach to the studied kaolinite collection showed that it includes both two-phase and one-phase samples. Figure 9 compares the ldp

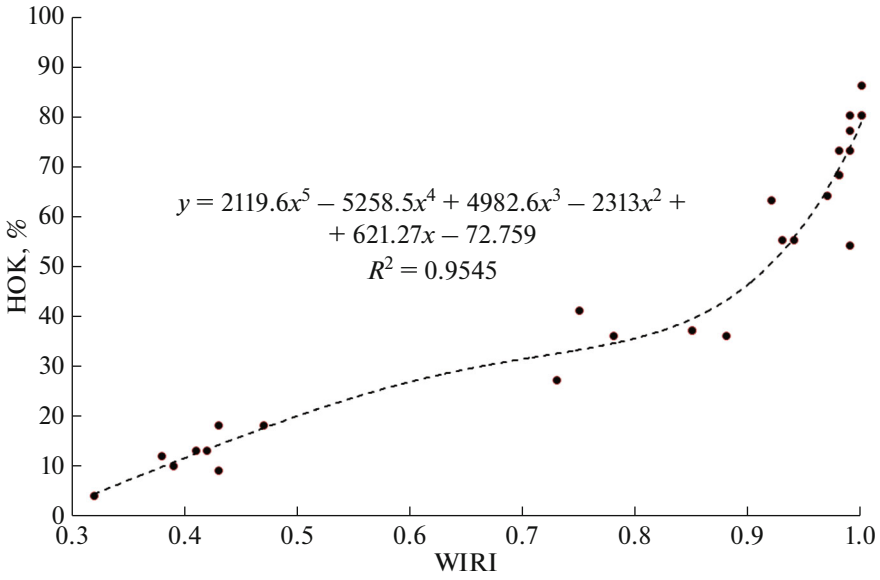

Fig. 7. Relationship between HOK and crystallinity index WIRI.

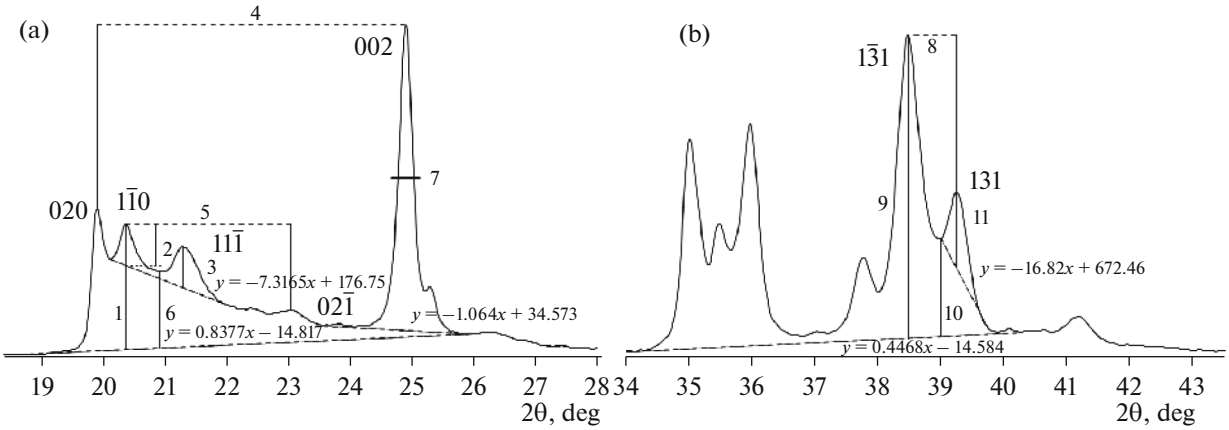

Fig. 8. Measurements used in the Expert System. (a) in the region of reflections 02*l*, 11*l* ((1) height of peak $1\bar{1}0$ measured from the diffractogram background line; (2) height of peak $1\bar{1}0$ measured from the background line drawn between reflections $1\bar{1}0$ and $11\bar{1}$; (3) height of peak $11\bar{1}$; (4) distance between reflections 020 and 002; (5) distance between reflections $1\bar{1}0$ and $02\bar{1}$; (6) height of background between reflections $1\bar{1}0$ and $11\bar{1}$; (7) FWHM–full width at half reflection 002; (b) in the region of reflections 20*l*, 13*l* ((8) distance between reflections $1\bar{3}0$ and 131; (9) height of peak $1\bar{3}1$; (10) height of background between reflections $1\bar{3}1$ and 131; (11) height of peak 131.

values obtained using the Expert System and the HOK values based on the modeling of experimental diffraction patterns. It shows that the HOK vs. ldp correlation is described well by the linear equation

$$\text{HOK}\ (\%) = 0.6836\,\text{ldp}(\%) + 9.4399 \qquad (9)$$

with $R^2 = 0.982$. All samples identified by Expert System as one-phase and low-ordered fell on the ordinate axis, while the modeling of their diffractograms showed the presence of the HOK phase (4–18%) (Fig. 9, Table 3). It should be noted that discrepancies in the estimation of the number of phases were also pointed out in (Plançon and Zacharie, 1990) based on the study of natural kaolinites using Expert System and the method of XRD pattern modeling (samples C3 and III-Mp in (Plançon and Zacharie, 1990, Table 1). On the other hand, Expert System predicts the ldp content greater than 100% for several samples from this collection (Keok-1, Keok-2, Keok1D, and Keok2D) (Fig. 9).

If we now plot the HOK and ldp correlation with HI on one plot, they are described by different regression curves with different correlation coefficients R^2

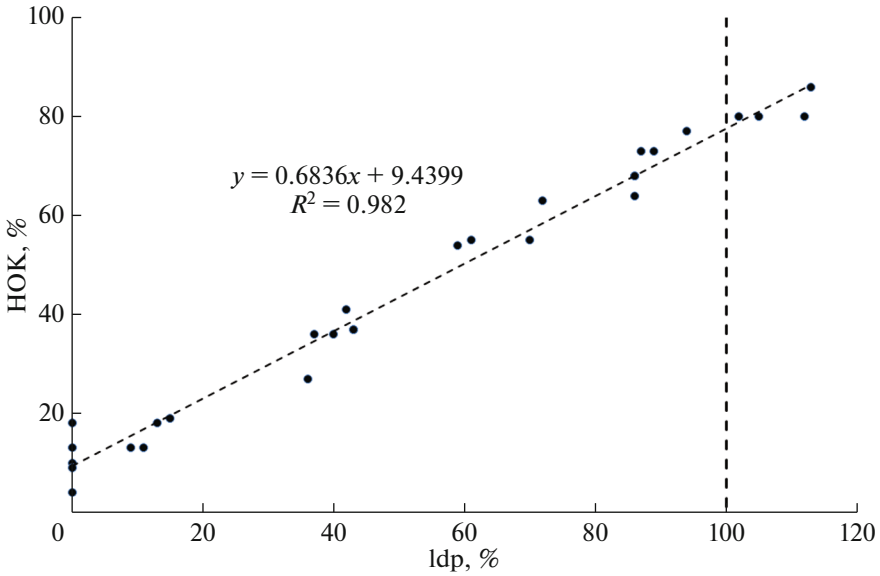

Fig. 9. Relationship between HOK and ldp.

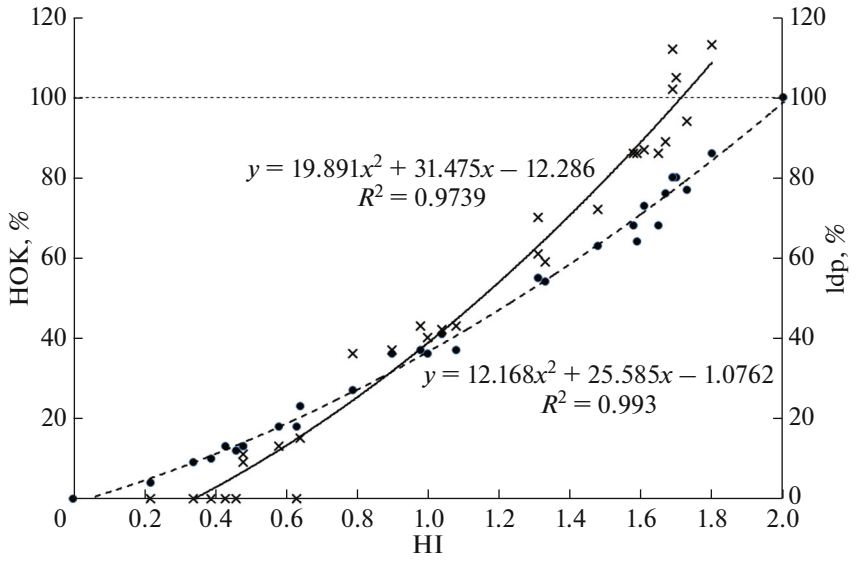

Fig. 10. Relationship of the Hinckley crystallinity index (HI) with values of HOK (black circles) and ldp (crosses).

$$\text{ldp (\%)} = 19.891\ \text{HI}^2 + 31.475\ \text{HI} - 12.286,\quad R^2 = 0.974 \qquad (10)$$

(cf. Eqs. (1) and (10)). The closest agreement between the HOK and ldp values is observed at HI ~ 1.00, whereas their values differ markedly in different directions at HI < 0.70 and HI > 1.30. If the regression curve of the HOK vs. HI correlation (Fig. 10) almost coincides with the origin, then Expert System predicts average HI ~ 0.3 for the one-phase low-ordered samples (ldp vs. HI correlation at ldp = 0, Fig. 10), with HI variations from 0.22 to 0.63 (Table 3). Taking the HOK values obtained by modeling experimental diffraction patterns as true, the corresponding ldp values at HI < 0.70 are underestimated and, conversely, overestimated at HI > 1.30 (Table 3, Fig. 10). These discrepancies can be caused by the following fact: Expert System was based on the analysis of diffraction patterns calculated for various models of the defect structures of kaolinite, whereas the HOK values for the analyzed samples were obtained by modeling their experimental diffractograms.

As already mentioned above, Expert System often predicts one-phase samples at small HI values (e.g., G5, S218, 5920, Bor-2, 6194, and KGa-2 with HI =

0.63–0.22). However, the HOK and ldp values are close for samples Im, Ma4, and 5914 with HI = 0.58–0.48 (Table 3). The largest difference between the HOK and ldp values (18%) was established for sample G5. Therefore, it is interesting to compare the simulation results of this sample for the two-phase and one-phase models. In Figs. 11a and 11b fragments of an experimental diffractogram of sample G5 in the 2θ region containing 02*l*, 11*l*, and 002 reflections are compared with diffraction patterns calculated for the two-phase and one-phase models. The corresponding structural parameters are given in Table 2. It should be noted that a comparison of the calculated diffraction patterns for both models in the entire 2θ region from reflection 001 to reflection 060 showed that they almost do not differ anywhere, except for the region highlighted in Figs. 11a and 11b with reflections 02*l*, 11*l* and 002. The two-phase model (Fig. 11a) almost lacks any significant differences between the experimental and calculated profiles of the compared patterns, except for a small intensity difference at ~22-23.5° 2θ, probably, due to the presence of a small diaspore admixture in the sample. Position of reflections $1\bar{1}0$, $11\bar{1}$, and $02\bar{1}$ on the diffractogram are determined entirely by the contribution of the HOK phase (close to the positions of these reflections for a perfect kaolinite), since the contribution from the LOK phase provides only high background scattering at these 2θ values. The profile factor characterizing the degree of discrepancy between the compared diffraction patterns (Rp = 8.17%). Notably large differences between the experimental and calculated patterns in this 2θ range (Fig. 11b) are observed in the case of a one-phase model. Due to an increase in the concentration of layer translations t_2 in the one-phase model (W_{t2} = 0.20, Table 2), as compared with their content in the HOK phase of the two-phase sample (W_{t2} = 0.02, Table 2), one can see a notable shift of reflection $02\bar{1}$ toward small 2θ angles (Fig. 11b). Consequently, profile factor for the compared patterns increases to Rp = 8.56%. According to (Plançon and Zacharie, 1990), Expert System uses this effect to identify the one-phase and two-phase samples. However, in the comparison of the calculated diffraction patterns for the two-phase and one-phase models with the diffractogram of sample G5, preference should likely be given to the two-phase model as better corresponding to the experimental pattern. Since Expert System identified this sample as one-phase, it cannot be considered a reliable method for the unambiguous structural interpretation of such samples.

DISCUSSION

Do one-phase samples exist?

Among all of kaolinite samples studied by the modeling of experimental diffraction patterns, we did not find any one-phase and highly defective sample. On the other hand, we also did not detect any one-phase and low-defective kaolinite. From the diffraction point of view, the two-phase low-ordered samples should exhibit relatively weak and wide (but notable) intensity modulations close in position to $1\bar{1}0$, $1\bar{1}0$, and $11\bar{1}$ reflections of kaolinite against the background of a wide and intense "hump" in the 19°–25° 2θ region, whereas the two-phase and highly ordered samples in this region should demonstrate a notable background scattering between the well-resolved kaolinite reflections 02*l* and 11*l*. It is rather easy to detect these features of diffractograms for kaolinite samples with 10 < HOK < 80, but much more difficult for samples with HOK < 10 and HOK > 80. At the same time, one-phase kaolinites of variable degrees of defect may exhibit diffraction effects close to those observed for the two-phase samples. As example, Fig. 12 shows fragments of the calculated diffraction patterns containing reflections 02*l*, 11*l*, and 002 for the two-phase and one-phase models, in which all structural parameters of individual phases are the same, except for the occurrence probabilities of layer translations W_{t1} and W_{t2}. As is evident from Fig. 12, for any one-phase kaolinite structure with the given W_{t1} : W_{t2} ratio, it is possible to choose such a ratio of HOK and LOK phases in the two-phase model that the calculated diffraction patterns for both models will differ by no more than 4.5%. Moreover, if we compare these patterns over the entire 2θ range from reflection 001 to 060, they coincide completely, except for the highlighted fragment in Fig. 12. Hence, diffraction methods averaging the structural characteristics of individual crystallites can be unsuitable for determining the structural heterogeneity of natural kaolinites. Therefore, it is not surprising that Expert System, as shown above, sometimes poorly identifies the two-phase samples with HOK < 20, taking them for the one-phase and highly defective. At the same time, the Hinckley index, as we saw above, turned out to be a very sensitive parameter for two-phase samples, both with high and low LOK phase content.

Based on the study of kaolinite samples by modeling experimental diffractograms, three samples (III-I, IV-L, and V-G) were classified as one-phase kaolinites in (Plançon et al., 1989, Fig. 1, Tables 1, 2). Diffraction patterns of these samples almost lack modulations of kaolinite reflections $1\bar{1}0$ and $11\bar{1}$, although the corresponding HI was estimated at 0.43, 0.32, and 0.18 based on these reflections (Plançon et al., 1989, Table 2). It is possible that these samples are also two-phase. This discrepancy can be related to the following fact: experimental diffractograms were simulated by these authors not simultaneously for the entire diffraction pattern, but separately in two selected fragments with reflections 02*l*, 11*l*, and 20*l*, 13*l* and without taking into account the contribution of basal reflections 002 and 003. Moreover, the authors improperly allowed different CSD sizes in the plane of *ab* layers

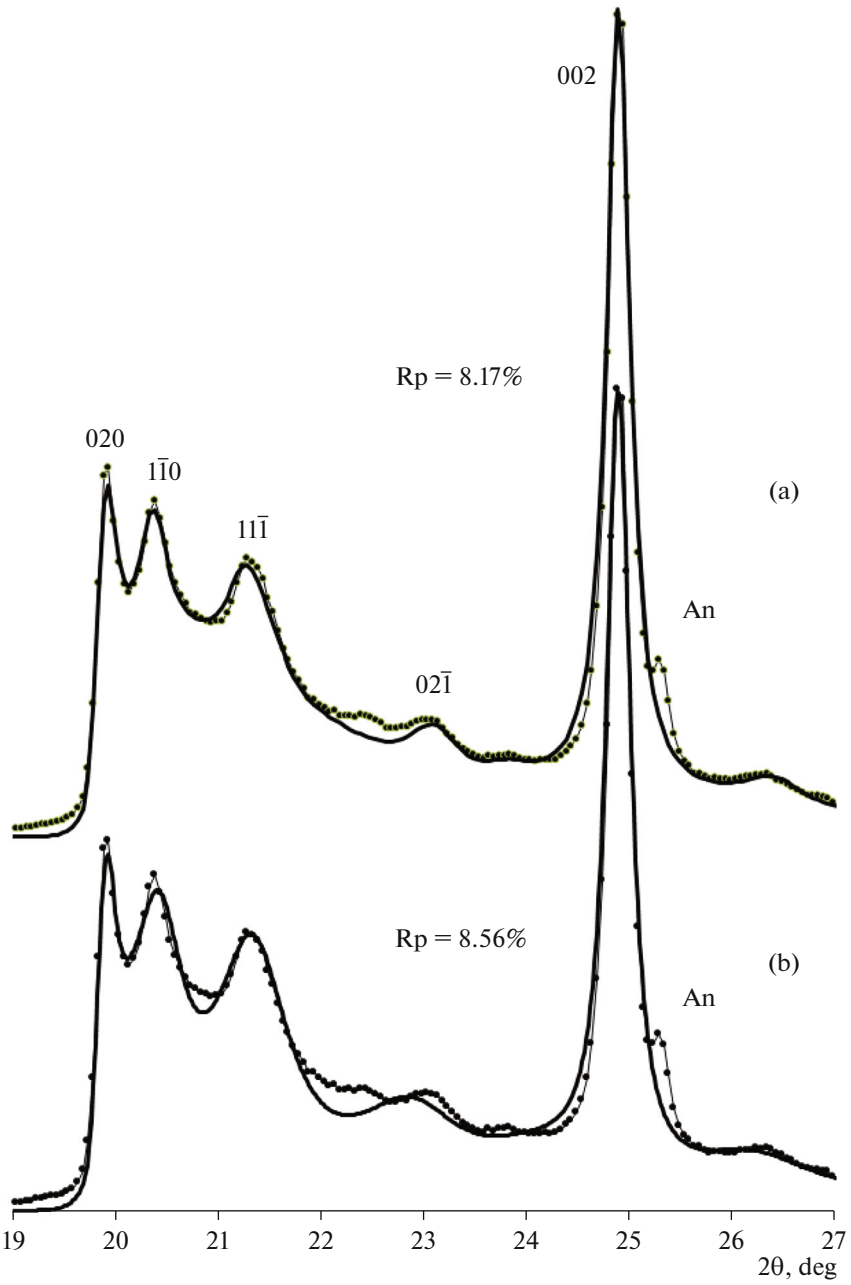

Fig. 11. Comparison of a fragment of the experimental diffractogram of sample G5 in the region of reflections 02*l* and 11*l* with the diffraction patterns calculated for the two-phase (a) and one-phase (b) model of the kaolinite defective structure (structural parameters of models are presented in Table 2; An—anatase).

when modeling individual fragments of diffractograms with indices 02*l*, 11*l* and 20*l*, 13*l* (Plançon et al., 1989, Table 2). Our collection of kaolinites lacked any sample, with the diffraction pattern showing only a "hump" of background scattering in the 02*l* and 11*l* reflection region without notable intensity modulations close to the positions of reflections 1$\bar{1}$0 and 11$\bar{1}$.

Obviously, the one-phase HOK can be considered a Keokuk sample, whose structure was refined by D. Bish and von Dreele by the Rietveld method. Its powder diffraction pattern lacks any background scattering between reflections 020, 1$\bar{1}$0, 11$\bar{1}$, and 1$\bar{1}\bar{1}$ (Bish and von Dreele, 1989, Fig. 2). According to our estimates, the HI value for this sample is ~2.00. If we assume that HOK = 100% for this sample, the corresponding point on the HOK versus HI plot (Fig. 2) almost coincides with the regression curve. Apparently, it can now be argued that the HI value for natural kaolinites varies from 0 to 2.00, and the corresponding HOK value ranges from 0 to 100%.

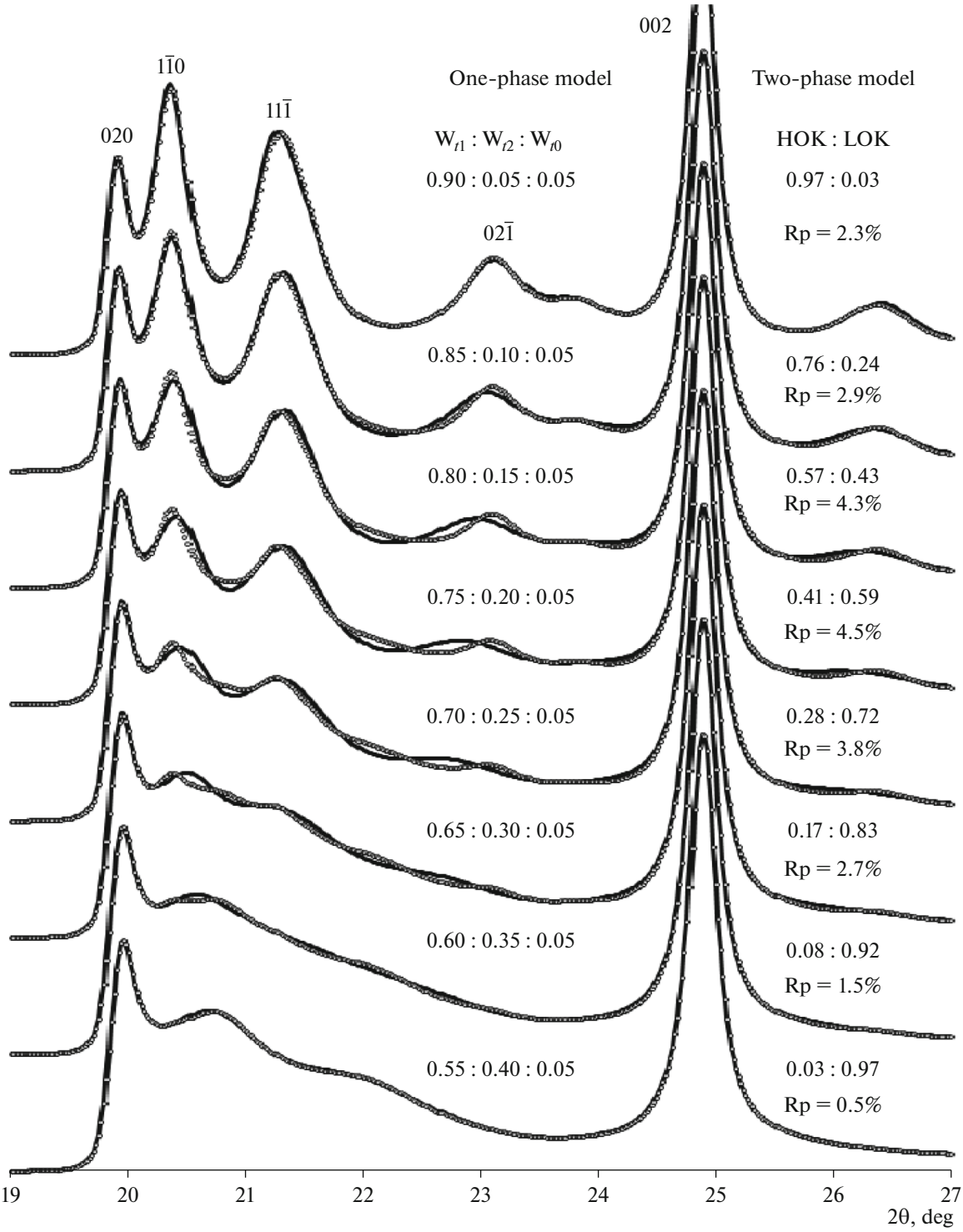

Fig. 12. Comparison of diffraction patterns in the region of reflections 02*l* and 11*l* calculated for the one-phase (solid line) and two-phase (circles) models of kaolinite defective structure. The content of layer translations in the one-phase model (W_{t1} : W_{t2} : W_{t0}) is shown in the figure near each curve. In the two-phase model of HOK and LOK, W_{t1} : W_{t2} = 0.98 : 0.02 and W_{t1} : W_{t2} : W_{t0} = 0.50 : 0.45 : 0.05, correspondingly; all remaining structural parameters of individual phases are similar in both models; the HOK : LOK ratio is shown near each curve. Rp—profile factor characterizes the discrepancy degree of diffraction patterns calculated for the one-phase and two-phase models.

Possible explanation of the formation of HOK and LOK phases in a single sample

Manifestation of enantiomorphism in kaolinite minerals was demonstrated experimentally by the methods of vacuum decoration and transmission electron microscopy on the growth patterns of elementary kaolinite layers with a thickness of 7Å (Samotoin, 2010; Samotoin and Bortnikov, 2014). These results indicate that both right- and left-handed triclinic kaolinite crystals are formed easily in nature, which cannot be distinguished by diffraction methods. At the same time, all known refinements of the kaolinite structure show that its 1 : 1 layers lack symmetry elements and are characterized by an oblique base-centered layered unit cell with $\gamma < 90°$, but at the same time contain a pseudo-mirror plane passing along the long diagonal of this cell (Bish, 1993; Bish and von Dreele, 1989; Drits and Kashaev, 1960; Neder et al., 1999; Sutch and Young, 1983; Zvyagin, 1960); i.e., identical atoms are located at close, but still different distances on both sides of this diagonal. At the same time, one should agree with the concept in (Bookin et al., 1989) that from the crystal-chemical and structural points of view, real distortions of the kaolinite layer allow only stacking faults related to the alternation of enantiomorphic right- and left-hand kaolinite fragments interrelated by a glide plane. Hence, the layers most likely have a real mirror plane in such defective 1 : 1 structures. Thus, the HOK phase in kaolinite samples is likely characterized by a triclinic structure, where 1 : 1 layers do not have a mirror plane and, therefore, only the ordered right- or left-handed crystals having only a few number of random stacking faults can grow. On the contrary, kaolinite layers in LOK phase crystals always have a mirror plane. Therefore, the left- and right-handed enantiomorphic fragments are formed easily in crystallites due to random defects in the stacking of identical layers related to the alternation of layer translations t_1 and t_2 in approximately equal proportions. Apparently, the different ratio of HOK and LOK phases in different samples depends on their genesis, geological setting, formation mechanism, and others.

Why is knowledge of the real kaolinite structure important for interpreting experimental data?

Recently, a combination of the synchrotron radiation XRD and X-ray/Neutron pair distribution function was used in (Lee and Xu, 2020) to determine the average and local structure of natural Murfreesboro kaolinite from the S.V. Bailey collection (Department of Geosciences, University of Wisconsin-Madison, USA). The aim of the work was to demonstrate the new possibilities of modern methods for studying the structure of exclusively dispersed mineral objects, for which the single-crystal methods cannot be applied. Probably, the choice of this sample was based on the firm belief of the authors that its structure is highly ordered and devoid of any defects. As already mentioned above, the two-phase kaolinite samples are characterized by a diffraction pattern, in which reflections 02*l* and 11*l* appear against the background of a wide and intense "hump" in the 19°–25° 2θ region. Exactly such intensity distribution is recorded in this region in the given sample (Lee and Xu, 2020, Fig. 5). Therefore, it can be assumed that the studied kaolinite is actually a two-phase variety containing both high-ordered (HOK) and low-ordered (LOK) phases. Determination of the HI value from their diffraction pattern (Lee and Xu, 2020, Fig. 5) showed that HI = 0.79. Using Eq. (1), we find that HOK = 26.5%. Hence, only one-third of crystallites in the sample have a perfect or almost perfect structure, while two-thirds of other crystallites are highly defective. It should be noted that the HOK and HI values, as well as diffraction pattern of the Murfreesboro sample almost coincide with the corresponding values for the international standard KGa-1 (The Source Clays Repository of The Clay Mineral Society) whose real structure and two-phase composition were confirmed by modeling its experimental diffraction pattern (Sakharov et al., 2016). Therefore, the results of application of these powder methods for a sample with a high content of stacking faults cannot be considered reliable.

ACKNOWLEDGMENTS

The authors express gratitude to O.V. Zakusina (Dorzhieva) and D.M. Korshunov who provided kaolinite samples for the study.

FUNDING

This work was accomplished under the State Task of the Geological Institute, Russian Academy of Sciences.

REFERENCES

Aparicio, P., Ferrell, R., and Galán. E., A new kaolinite order index based on XRD profile fitting, *Clay Miner.*, 2006, vol. 41, pp. 811–817.

Aparicio, P. and Galán, E., Mineralogical interference on kaolinite crystallinity index measurements., *Clays Clay Miner.*, 1999, vol. 47, pp. 12–27.

Bailey, S.W., *Kaolin Genesis and Utilization (A Collection of Papers Presented at the Keller '90 Kaolin Symposium)*, Murray, H.H., Bundy, W.M., and Harvey, C.C., Eds., Boulder: Clay Miner. Soc., 1993, pp. 25–42.

Bailey, S.W., Polytypism of 1 : 1 layer silicates, in *Hydrous Phyllosilicates (Exclusive of Micas)*, Bailey, S.W., Ed., Chantilly: Miner. Soc. Am., 1988, vol. 19, pp. 9–27.

Bish, D.L. and von Dreele R.B., Rietveld refinement of non-hydrogen atomic positions in kaolinite., *Clays Clay Miner.*, 1989, vol. 37, pp. 289–296.

Bookin, A.S., Drits, V.A., Plançon, A., and Tchoubar, C., Stacking faults in kaolin-group minerals in the light of real

structural features, *Clays Clay Miner.*, 1989, vol. 37, pp. 297–307.

Brindley, G.W., Kao, C.C., Harrison, J.L., Lipsicas, M., and Raythatha, R., Relation between structural disorder and other characteristics of kaolinites and dickites, *Clays Clay Miner.*, 1986, vol. 34, pp. 239–249.

Brindley, G.W. and Robinson, K., The structure of kaolinite, *Miner. Mag.*, 1946, vol. 27, pp. 242–253.

Chmielová, M. and Weiss, Z., Determination of structural disorder degree using an XRD profile fitting procedure: Application to Czech kaolins, *App. Clay Sci.*, 2002, vol. 22, pp. 65–74.

Drits, V.A., Zviagina, B.B., Sakharov, B.A., Dorzhieva, O.V., and Savichev, A.T., New insight into the relationships between structural and FTIR spectroscopic features of kaolinites, *Clays Clay Miner.*, 2021, vol. 69, pp. 366–388.

Drits, V.A. and Kashaev, A.A., An X-ray diffraction study of a single crystal of kaolinite, *Sov. Fiz. Kristallogr*, 1960, vol. 5, pp. 207–210.

González, I., Aparicio, P., and Galán, E., Correlation between the most frequently used XRD crystallinity indices for kaolinite: their accuracy and reproducibility, in *Clays for our Future*, Kodama H., Mermut, A.R., and Torrance, J.K., Eds., Ottawa: ICC-97 Org. Comm., 1999, pp. 367–374.

Hinckley, D.N, Variability in "crystallinity" values among the kaolin deposits of the coastal plain of Georgia and South Carolina, *Clays Clay Miner.*, 1963, vol. 11, pp. 229–235.

Kogure, T., Stacking disorder in kaolinite revealed by HR-TEM: a review, *Clay Sci.*, 2011, vol. 15, pp. 3–11.

Kogure, T. and Inoue, A., Determination of defect structures in kaolin minerals by high-resolution transmission electron microscopy (HRTEM), *Am. Miner.*, 2005, vol. 90, pp. 85–89.

Kogure, T., Johnston, C.T., Kogel, J.E., and Bish, D., Stacking disorder in a sedimentary kaolinite, *Clays Clay Miner.*, 2010, vol. 58, pp. 63–72.

Lee, S. and Xu, H., Using complementary methods of synchrotron radiation powder diffraction and pair distribution function to refine crystal structures with high quality parameters – A review, *Minerals*, 2020, vol. 10, p. 124.

Murray, H.H., Structural variation of some kaolinites in relation to dehydroxylated halloysite, *Am. Miner.*, 1954, vol. 39, pp. 97–108.

Neder, R.B., Burghammer, M., Grasl, Th., Schulz, H., Bram, A., and Fiedler, S., Refinement of the kaolinite structure from single-crystal synchrotron data, *Clays Clay Miner.*, 1999, vol. 47, pp. 487–494.

Plançon, A. and Tchoubar, C., Determination of structural defects in phyllosilicates by X-ray powder diffraction-II. Nature and proportion of defects in natural kaolinites, *Clays Clay Miner.* 1977, vol. 25, pp. 436–450.

Plançon, A. and Zakharie, C., An expert system for the structural characterization of kaolinites, *Clay Minerals*, 1990, vol. 25, pp. 249–260.

Plançon, A., Giese, R.F., Snyder, R., Drits, V.A., and Bookin, A.S., Stacking faults in the kaolin-group mineral defect structures of kaolinite, *Clays Clay Miner.*, 1989, vol. 37, pp. 203–210.

Range, K.J. and Weiss, A., Über das Verhalten von Kaolinitit bei Hohen Drücken, *Ber. Deut. Keram. Ges.*, 1969, vol. 46, pp. 231–288.

Sakharov, B.A., Drits, V.A., McCarty, D.K., and Walker, G.M., Modeling of powder X-ray diffraction patterns of the Clay Minerals Society kaolinite standards: KGa-1b and KGa-2, *Clays Clay Miner.*, 2016, vol. 64, pp. 314–333.

Samotoin, N.D., Enantiomorphism of kaolinite: Manifestation at the levels of elementary layer and microcrystals, *Cryistallogr. Repts.*, 2011, vol. 56, pp. 327–334.

Samotoin, N.D., Right- and left-hand microcrystals of kaolinite and their natural abundance, *Dokl. Earth Sci.*, 2010, vol. 431, pp. 399–402.

Samotoin, N.D., and Bortnikov, N.S., Growth surface topography of kaolinite-group minerals and their simulation based on the regular sequence of enantiomorphic layers, *Crystallogr. Repts.*, 2014, vol. 59, pp. 594–606.

Stoch, L., *Mineraly Ilaste*, Warsaw: Geol. Publ., 1974, pp. 186–193.

Stoch, L. and Sikora, W., *Określenie stopnia uporządkowania struktury mineralów grupy kaolinite*, Krakowie: Spraw. Pos. Kom. Nauk, 1966, pp. 651–654.

Suitch, P.R. and Young, R.A., Atom position in highly ordered kaolinite, *Clays Clay Miner.*, 1983, vol. 31, pp. 357–366.

Wojdyr, M., Fityk: a general-purpose peak fitting program, *J. Appl. Crystall.*, 2010, vol. 43, pp. 1126–1128.

Zvyagin, B.B., Electron diffraction determination of the structure of kaolinite, *Sov. Fiz. Kristallogr.*, 1960, vol. 5, pp. 32–41.

Translated by D. Sakya